Experimental Facility for Measuring Aircraft Inlet/Engine Radar Cross Section

S. Wong, E. Riseborough and G. Duff
Defence R&D Canada – Ottawa
3701 Carling Ave., Ottawa, Ontario
Canada K1A 0Z4

K. K. Chan
Chan Technologies Inc.,
15 Links Lane, Brampton, Ontario
Canada L6Y 5H1

ABSTRACT

A full-size aircraft engine-duct mock-up experimental apparatus has been built to collect cavity radar cross section (RCS) data on aircraft engine inlets. The engine-duct structure is made up of a cylindrical duct with a single fan stage consisting of 30 generic straight fan blades. Experimental results indicate that the azimuthal RCS patterns from the engine-duct are quite complex. Numerical computations using a commercial RCS prediction code are compared with the measured data. The comparisons between measured and computed data have highlighted some of the problems and difficulties currently encountered in cavity RCS modelling. These results indicate that engine-duct RCS modelling is a very challenging problem.

1.0 INTRODUCTION

A recent research effort in Non-Cooperative Target Recognition within the Combat ID community involves the development of a synthetic target signature database for target classifiers. For various technical reasons, a synthetically generated database is regarded as the most practical way of fielding an operational target classifier system [Ref. 1]. Synthetic target signatures are computed using high frequency electro-magnetic radar cross-section (RCS) prediction codes. There has been a great deal of research activities in recent years focusing on cavity RCS modelling of aircraft inlet/engine interface. It has been known that the inlets of aircraft produce a significant RCS contribution to the overall RCS of an aircraft [Ref. 2]. Therefore, cavity RCS computation should be an integral part of the synthetic signature generation process of aircraft.

Although there are many in-depth cavity modelling efforts being conducted in the Combat ID community [Ref. 3], there is still a lack of readily available experimental data to validate the numerical analyses. Moreover, there is virtually no experimental data on full-size engine-duct model available, even in the open literature. In order for the numerical modelling results to be deemed as credible and reliable, they must be validated by experimental data. Sub-scale inlet model data have been found to be unreliable as a predictor of full-scale results [Ref. 4]. Hence for practical aircraft inlet RCS modelling, full-scale experimental data are desirable and pertinent to synthetic target signature generation. Furthermore, we are developing a numerical model for aircraft engine/inlet RCS based on the modal method [Ref. 5, 6, 7]. This modal approach in

Paper presented at the RTO SET Symposium on "Target Identification and Recognition Using RF Systems", held in Oslo, Norway, 11-13 October 2004, and published in RTO-MP-SET-080.

modelling the radar backscattering permits computations on full-size engine-duct structure. To overcome the shortage problem of measured data, we have designed and built a full-size generic aircraft engine-duct mock-up for collecting cavity RCS data.

Computations from a commercial RCS prediction code are compared with the measured data. This permits an assessment of the capability of the current high frequency electro-magnetic RCS computational technology for predicting cavity RCS from targets.

2.0 EXPERIMENTAL SET-UP OF THE ENGINE-DUCT MOCK-UP

All components in the engine-duct mock-up are made of simple geometrical shapes. The inlet duct is a metallic cylinder with a 0.7 m diameter. The length of the duct can be varied up to 2m. The roundness of the cylindrical duct is reinforced by mounting the duct in a wooden circular brace structure. The "engine" is represented by a single fan stage consisting of 30 fan blades. The fan blades are simple, flat metal stripes and have dimensions of 24.6 cm in length, 10.4 cm in width and 0.16 cm in thickness. They are cut using a stencil to ensure all the fan blades are identical. The fan shaft and the nose cone are machined out of solid metal blocks for symmetry and structural rigidity. Great care has been exercised in mounting the fan blades onto the fan shift so that the fan stage is as symmetrical as possible. Each blade is set at a 45-degree angle with respect to the axial axis of the duct. An exposed view of the engine-duct CAD (Computer Aided Design) model is shown in Figure 1. The simple geometry of the engine-duct structure allows measured data to be compared with numerical results in a meaningful and definitive manner. Moreover, the simple geometry of the engine-duct mock-up permits the structure to be built with a greater degree of symmetry. It will be seen later that the symmetry of the experimental apparatus is crucial to collecting meaningful measured data.

The engine-duct mock-up is mounted on a rotating platform. A computer controlled stepping motor is used to drive the rotating platform. The rate of rotation can be varied but is nominally set at 1 degree/s for the RCS measurements. The rotational rate is consistent to within 2 seconds over a 180-second duration over many trial runs. With the stepping motor controlled by the computer, the position of the rotating platform can be reset to the original position almost perfectly. Any positional error in the re-setting of the turntable comes from the backlash of the gearing system. But the backlash error is very small and it takes many runs before a 1 to 2-degree re-setting error is noticed. RCS measurements of the engine-duct mock-up are collected at X-band radar frequencies. The radar frequency can be varied from 8.9 GHz to 9.4 GHz. The radar pulse repetition rate (PRF) is operated at 1kHz (i.e., 1000 measured data points per second) and the received radar signals have a HH polarization.

To ensure that the backscattered radar signal collected is returning from inside the duct only, the exterior of the engine-duct mock-up is covered by radar absorbing material (RAM). A photo of the engine-duct mock-up is shown in Figure 2. The RAM tiles are effective in the 8 to 10 GHz radar frequency region. A background check is conducted to verify that no spurious radar return is detected from the engine-duct. This is done by covering the duct entrance with RAM tiles and a RCS measurement is made by rotating the engine/inlet mock-up from –60 to +60 degrees in the azimuth direction (i.e., horizontally). The background RCS measurement is shown in Figure 3. It can be seen that the radar return is fairly constant over the 120- degree scanned azimuth angle, indicating that there is no spurious reflection from the engine-duct structure.

3.0 RCS MEASUREMENTS AND COMPUTATIONS FROM A SIMPLE DUCT

The duct is initially terminated with a flat plate only; i.e., no fan assembly inside the duct. As a first step, the flat plate termination offers a simpler engine duct geometry that makes it easier for comparing the RCS results

between measured and numerical data. This helps to establish a definitive reference to determine whether the basic scattering processes are being modelled reasonably in the numerical RCS code. An azimuthal RCS measurement of the engine duct is made, scanning from –60 to +60 degrees. The terminating flat plate is located 1m from the duct entrance. The radar frequency is at 8.9 GHz. Figure 4 (solid curve) shows the measured RCS of the engine duct as a function of azimuth angle. The flat plate is then moved back to 1.9m from the duct's entrance and another RCS measurement is made. The azimuthal RCS scan is shown in Figure 5 (solid curve). In both Figures 4 and 5, the RCS peaks on both sides of the zero azimuth-angle can be viewed as side lobes of the circular aperture Airy function of the flat plate, modified by reflections off the wall of the duct. Note that the measured RCS scans are quite symmetrical with respect to the zero azimuth-angle. The signal-to-noise ratio of the measured RCS signal is quite good. The signal is as much as 30dB above the noise floor in comparing with the background noise scan as shown in Figure 3.

A commercial electromagnetic RCS prediction code is used to compute the backscattered RCS from the duct. The RCS code employs the shoot-and-bounce ray tracing technique to compute the backscattered RCS from an object. The dashed curves in Figures 4 and 5 show the computed RCS of the duct with a terminating flat plate as a function of azimuth angle. It can be seen that the computed RCS patterns compare quite well with the measured data up to the first couple of major side lobes on both the positive and negative sides with respect to the zero azimuth-angle. As the azimuth angle is becoming more oblique, the RCS drops abruptly by more than 10dB in both the measured and computed RCS and the RCS patterns in these regions are no longer in agreement between the measured and computed data. However, it does not seem likely that the mismatches at large oblique azimuth angles are due to signal-to-noise issue in the measured data. The measured RCS values at large azimuth angles are still at least 10 dB above the noise floor as evident by comparing the measured RCS scans in Figures 4 and 5 to the noise floor reference as shown in Figure 3. Thus, the comparative results indicate that the computed RCS at large azimuth angle is becoming less accurate.

4.0 RCS MEASUREMENTS AND COMPUTATIONS WITH FAN ASSEMBLY

The fan assembly, i.e., fan blades and nose cone, is inserted in the cylindrical duct and is placed 1.9m inside the duct. The duct is still terminated with a flat plate as the last element inside the duct. RCS measurements are taken at a radar frequency of 8.9 GHz. The results are shown in Figure 6. Figure 6a shows the RCS of the engine-duct mock-up with the fan assembly placed at an arbitrary initial position. The fan assembly is then rotated 10 fan blades over in a clockwise direction. Another RCS measurement is made and the RCS result is shown in Figure 6b. Figures 6c, and 6d correspond to RCS measurements with the fan assembly rotated 20, and 25 blades with respect to the initial position as given in Figure 6a. These experimental results reveal that the azimuthal RCS patterns with the fan stage in the duct are much more complex than a simple duct and the RCS amplitude scintillates very rapidly as the azimuth angle of the engine-duct is changed by only a very minute amount. Furthermore, the results displayed in Figure 6 also indicate that the RCS patterns are somewhat different when taken at different fan positions.

Intuitively, one would expect that these RCS patterns to be identical since the fan assembly is supposed to be symmetrical upon rotation. But the differences in the RCS patterns persist despite diligent efforts trying to make the fan assembly as symmetrical as possible mechanically. However, the RCS pattern is readily reproducible when the fan assembly is returned to any of the four previous specific positions. Thus, it appears that the backscattered RCS pattern from the engine-duct is very sensitive to the symmetry of the fan assembly. In spite of the apparent differences among the four RCS plots in Figure 6, all the RCS peaks occur at the same positions among the four different fan positions. Only the amplitudes of the RCS peaks fluctuate when the fan assembly is rotated. This is shown in the superposition of the four RCS plots in Figure 7 (light solid curves).

The experimental results also reveal that the measured RCS patterns are asymmetric in the azimuth scan. There are more peaks recorded between –60 to 0 degrees than between 0 to +60 degrees. This asymmetry may be attributed to a couple of factors. Firstly, the elevation angle of the engine-duct's azimuthal plane may not be horizontal with respect to the radar transmitter/receiver (i.e., elevation angle is not zero). In other words, the engine-duct may be slightly tilted upward or downward. It is very difficult to align the engine-duct perfectly to the radar. In fact, non-zero elevation angle will be the norm in virtually all real data from in-flight aircraft. Secondly, the fan stage may not be as symmetrical as we would like it to be. The air gaps between the tips of the fan blades and the wall of the duct may not be uniform among the 30 blades. At 9 GHz, the tolerance for any spatial non-uniformity is about 0.002m (i.e., 1/16 λ). This amount of tolerance has not likely been met during the mounting of the fan blades onto the fan shaft. In addition, because the fan blades are made out of long, thin metal strips and they are anchored only at one end (e.g., at the fan shaft), some of the fan blades may be warped slightly due to gravity, by more than the 0.002m tolerances.

Numerical computations of the fan assembly in the duct are performed using the same parameters as the experimental set-up. The computed RCS as a function of azimuth angle is shown by the dashed curve in Figure 7. It can be seen that the computed RCS scan does not agree well at all with the measured data. The computed RCS amplitude tapers off steadily with increasing azimuth angle in both positive and negative directions. The failure in predicting the RCS amplitude correctly, especially at large oblique azimuth angles is a consequence of the shoot-and-bounce ray (SBR) tracing method employed in many of the RCS prediction codes. At large oblique azimuth angles, some of the input rays in the SBR method are lost in the duct and never contribute to the backscattering RCS [Ref. 8]. This is confirmed by monitoring the ray tracing statistics in the numerical computations. It is found that a large percentage of the input rays are lost in the computation as the azimuth angle becomes more oblique.

RCS measurements are also conducted at three different radar frequencies, 8.9 GHz, 9.1 GHz and 9.4 GHz. These are shown in Figure 8. The measured data reveal that the RCS patterns are quite different, indicating that radar backscattering from the engine-duct is very dependent on the radar frequency. The computed RCS at 9.4 GHz is shown in Figure 9. It can be seen that it does not match well with the measured one (i.e., Figure 8c). Furthermore, the RCS scan computed at 9.4 GHz looks very similar to the one that is done at 8.9 GHz as shown in Figure 7 (dashed curve). There is virtually no frequency dependence in the computed outputs. These results indicate that the current RCS prediction technology may still need more developmental efforts.

5.0 CONCLUSIONS

Cavity RCS measurements are conducted using a full-size engine-duct experimental mock-up. These RCS measurements indicate that the backscattering of radar radiation inside a engine-duct cavity structure is very complex. Experimental results reveal that the RCS is very sensitive to even a small change in the azimuth angle and to small mechanical asymmetry of the engine components. The RCS is also dependent on the radar frequency used. These factors pose some interesting challenges to the numerical modelling of engine-duct cavity RCS.

RCS prediction codes based on the shoot and bounce ray tracing method do not appear to be adequate for computing cavity RCS of complex structures such as aircraft engine inlets. Better numerical methods will have to be developed to model the cavity RCS accurately. This could be a critical area in the pursuit of developing realistic synthetic target signatures for target identification/recognition.

REFERENCES

[1] R. van der Heiden, F. C. A. Groen and L. J. van Ewijk, " Aircraft Recognition with Radar Range Profiles using a Synthetic Database", RTO Meeting Proceedings 40, "High resolution Techniques", NATO RTO, Neuilly-sur-Seine, Cedex, France, pp. 57-1 to 57-8, November 1999.

[2] H. T. Anastassiu, "A Review of Electromagnetic Scattering Analysis for Inlets, cavities and Open Ducts", pp.27-40, IEEE Antennas and Propagation Magazine, vol. 45, no. 6, December 2003.

[3] G. H. Goldman, "Characterization of the Effects of Cavities and Canopies on Radar Target Signatures", US Army Research Laboratory, Adelphi, MD, ARL-TN-154, February 2000.

[4] Bill Sweetman, "How LO can you get", Jane's International Defense Review, pp.20-22, January 2002.

[5] K.K. Chan and S. Wong, "Modal Approach to RCS computation of Electrically Large Inlets", IEEE AP-S International Symposium, pp.114-117, San Antonio, US, June 2002.

[6] K.K.Chan and S. Wong, "Accurate RCS Prediction of Electrically Large Jet Inlets and Engines", International Conference on Antennas and Propagation, Session 4b, Exter UK, April 2003.

[7] K.K. Chan, S. Wong and E. Riseborough, "Accurate Radar Cross Section Modelling of Jet Inlets and Engines", NATO Symposium on " Target Identification and Recognition Using RF Systems", Paper P16, Oslo, Norway, October 2004.

[8] A. Mackay, "Application of chaos theory to ray tracing in ducts", IEE Proc.- Radar, Sonar and Navigation, pp.298-304, vol.146, no.6, December 1999.

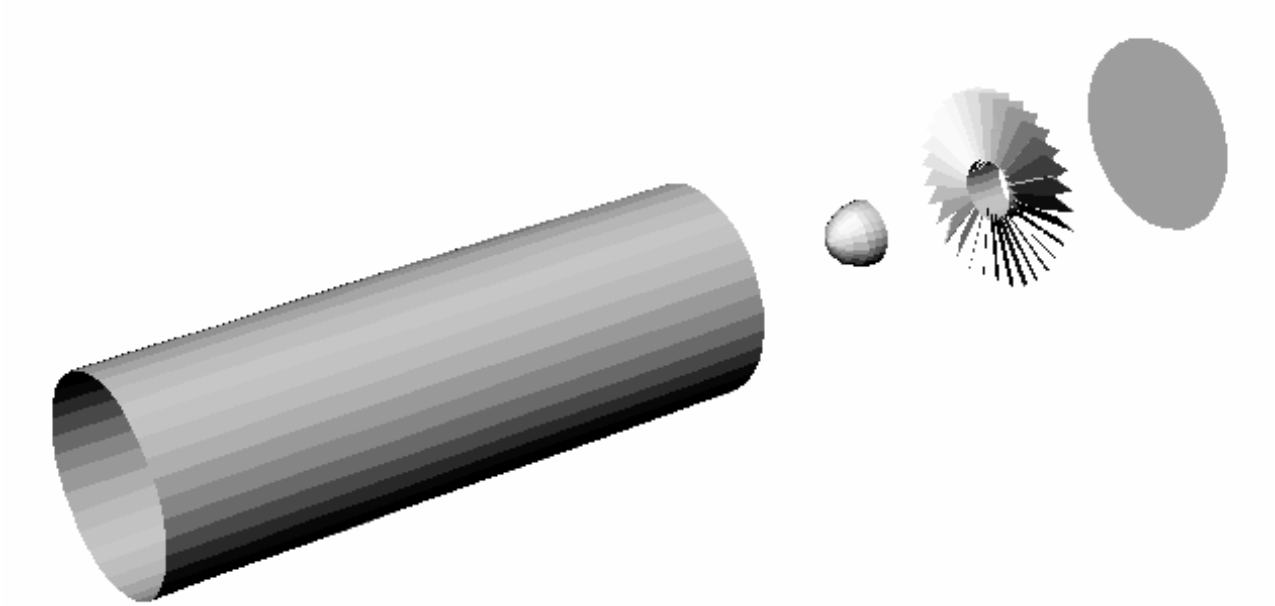

Figure 1 An exposed view of the engine-duct CAD model. From left to right: duct, nose-cone, fan stage and fan shaft, flat plate.

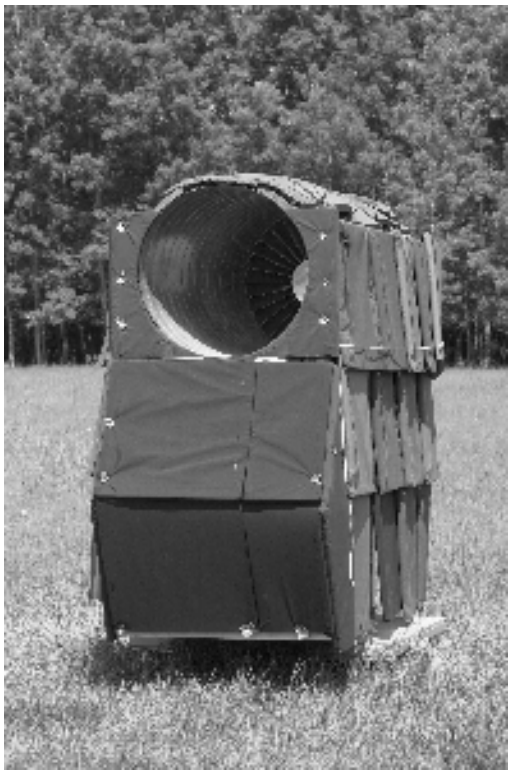

Figure 2 A picture of the full-size engine-duct mock-up with RAM tiles covering the exterior of the experimental set-up.

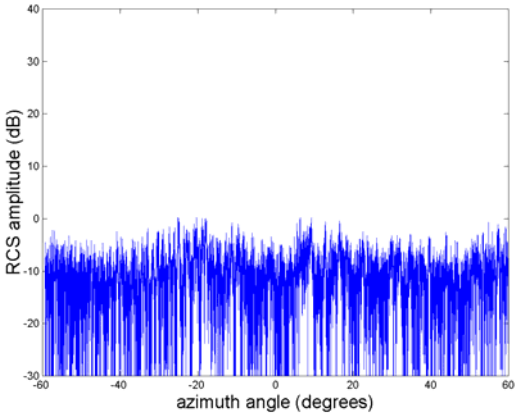

Figure 3 Background RCS measurement of the engine-duct mock-up. Radar frequency = 8.9 GHz.

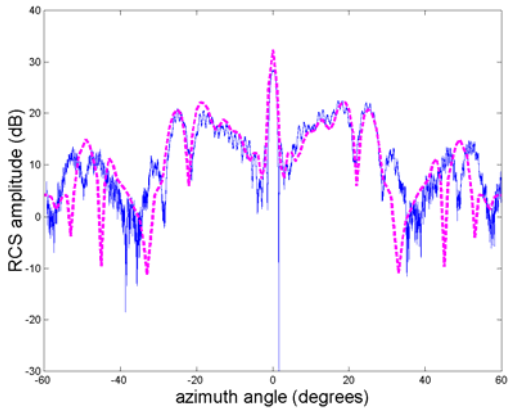

Figure 4 RCS as a function of azimuth angle for a cylinder with a terminating flat plate located 1m inside the duct. Solid curve = measured; dashed curve = computed.

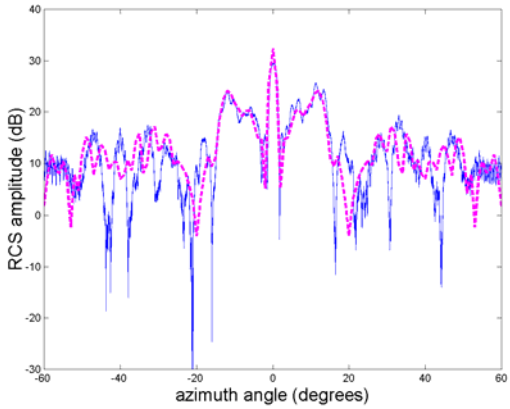

Figure 5 RCS as a function of azimuth angle for a cylinder with a terminating flat plate located 1.9m inside the duct. Solid curve = measured; dashed curve = computed.

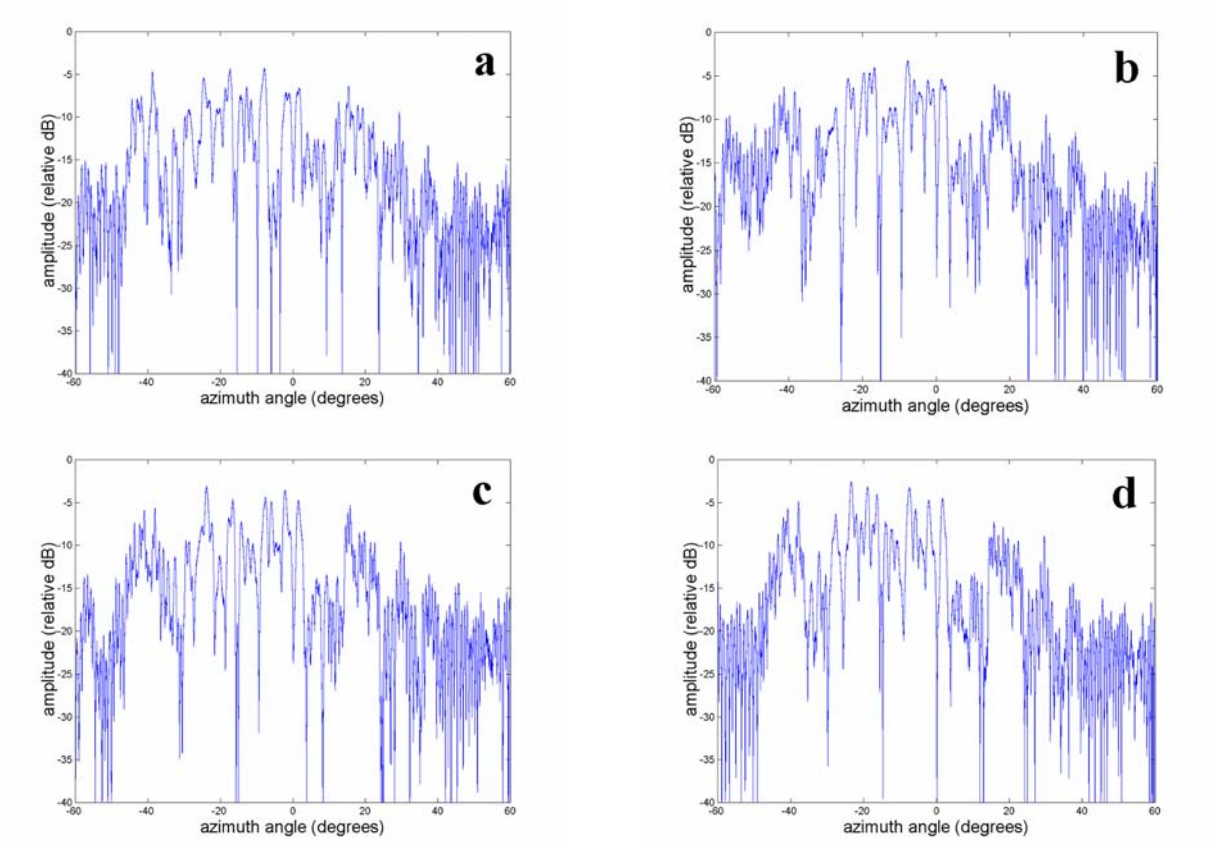

Figure 6 Measured RCS as a function of azimuth angle. Fan assembly is 1.9 m inside duct: a) reference position, rotated b) 10 fan blades, c) 20 fan blades, d) 25 fan blades counter-clockwise from reference position. Radar frequency = 8.9 GHz.

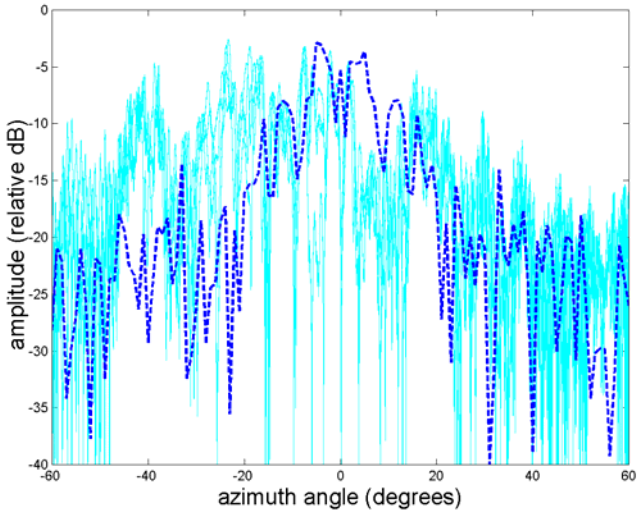

Figure 7 Light solid curve: superposition of the four RCS scans in Figure 6. Dashed curve: computed RCS as a function of azimuth angle. Radar frequency = 8.9 GHz.

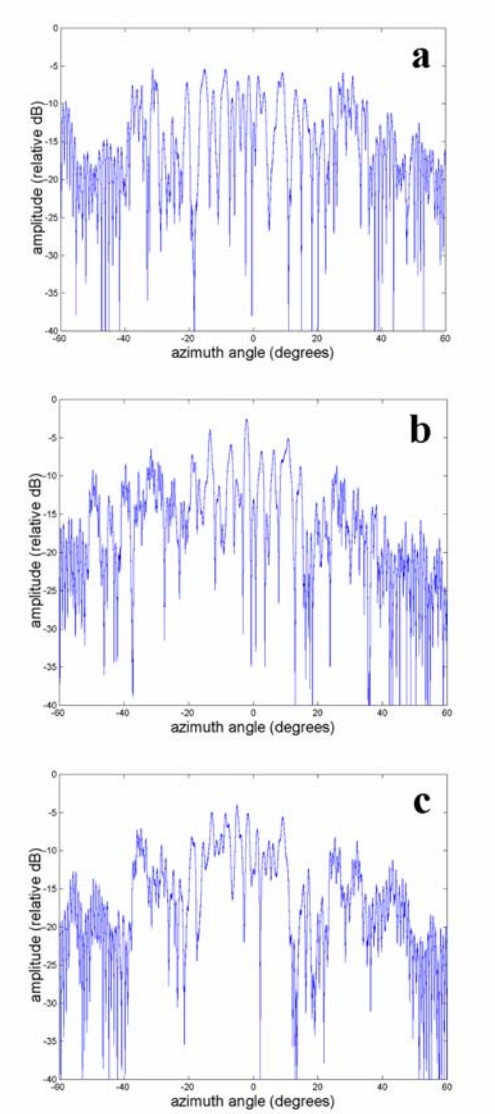

Figure 8 RCS as a function of azimuth angle measured at radar frequency: a) 8.9 GHz, b) 9.1 GHz, c) 9.4 GHz.

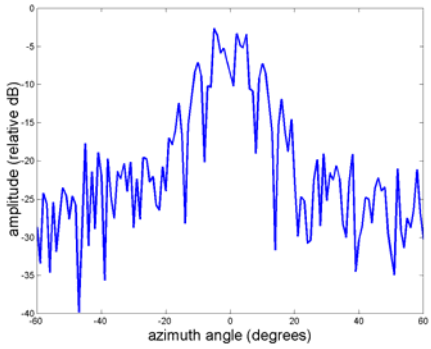

Figure 9 Computed RCS as a function of azimuth angle at 9.4 GHz.